Academic Journal of Science and Technology
ISSN: 2771-3032 | Vol. 9, No. 2, 2024

Research on the Characteristics of Stirring Flow Field of Flotation Separator Based on PIV Technology

Sijin Yu, Xiangyong Liao, Qiu Jing

School of Mechanical Engineering, Sichuan University of Science & Engineering, Yibin 643000, China

Abstract: In order to explore the distribution characteristics and characteristics of the internal flow field of the flotation machine, and to understand the variation law of the flow field parameters in the process of the internal flow field of the flotation machine, particle image velocimetry was used to measure the flow field of the flotation machine, and four groups of sections were designed, each group of sections had four different revolutions, and there were 16 experimental groups in total. The results show that the vertical plane of the flow field of flotation machine can be roughly divided into four areas. The flow field level of the flotation machine can also be divided into three areas. The effect of rotating speed on the average circulating speed of flotation machine was studied. This paper analyzes the statistical law of vorticity distribution in the internal flow field of flotation machine and the relationship between average speed and rotating speed, and establishes the probability model and influence analysis model related to it.

Keywords: PIV; Flotation machine; Velocity field; Vorticity.

1. Introduction

Flotation technology is based on adjusting the physical and chemical properties of mineral particles, separating useful minerals from ores, attaching them to bubbles, and then floating with bubbles to become foam products, so as to achieve the separation of useful minerals from other minerals [1][2]. Since the development of flotation cells, they can be roughly divided into four categories according to the different separation methods: pneumatic type, mechanical agitation type, reaction-separator and flotation column. In the past 100 years, despite the rapid development of flotation machines, mechanical stirring flotation machines still dominate the industry due to their maturity and practicability [2][3]. In this paper, in order to study the distribution characteristics and flow field characteristics of the flotation cell during stirring, the speed characteristics of the stirring flow field of the LZFD flotation cell were tested by laser PIV technology, and the data fitting of the flow field was carried out according to the experimental data, so as to provide a basis for the selection of the operating speed of the impeller and the improvement of the structure.

2. Experiment

2.1. Experiment quipment

The test device is a three-dimensional PIV measurement device produced by Dantec Dynamics in Denmark, which mainly includes four parts: light source system, image acquisition system, PIV synchronization system and image analysis system [4], as shown in Figure 2-1. The container containing the solution in the experiment is a hollow rectangular body assembled and glued together by transparent plexiglass, and the specifications are: In the experiment, the tracer particles were rhodamine B fluorescent polymer particles, which had good tracerability, scattering and follow-up properties of the convective field. The depth of the mixing solution is 430 mm. The motor selects a stirring motor with a rated power of 100W. One stepper motor speed controller. LZFD flotation machine (built-in stirring impeller with a diameter of 45mm).

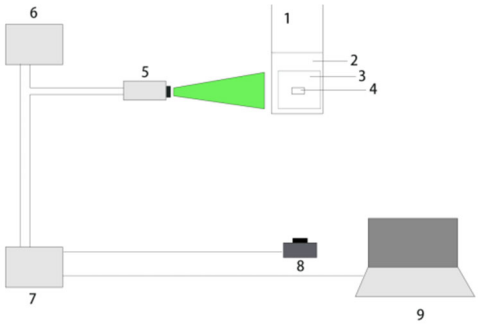

Figure 1. Schematic diagrams of experiment

2.2. Protocol

Select the vertical cross-section of the centerline of the horizontal section of the rectangular container as the reference cross-section, as shown in Figure 2-2, make it a 0-0 cross-section, and then extend it downwards to a depth of 20mm, 40mm, and 60mm for the shooting cross-section. Figure 2-3 shows that the PIV shooting area is 70 mm away from the bottom surface of the liquid, 60 mm from the left wall, and 240 mm high. In order to obtain the changes of the flotation machine at different speeds of the same shooting cross-section, the speed of the stirring impeller was preliminarily proposed to be 800、1200、1600、2000 four gears for recording and observation. As shown in Figure 2-4, the impeller axis is set to L2, the left side of the axis is set to L1, and the right side of the axis is set to L3 at 120mm.

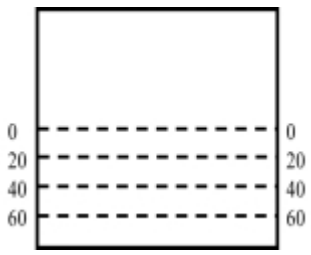

Figure 2. Schematic diagram of the horizontal section of the flotation machine box

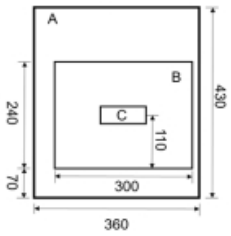

A-LiquidB-Camera

Figure 3. Schematic diagram of the PIV shooting area

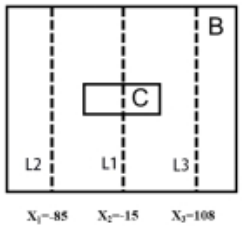

C-impeller

Figure 4. Schematic diagram of axis selection

3. Results

3.1. Plots and Models

In order to further explore the characteristics of flow field motion, the vorticity is analyzed.Figures 3-6 and 3-7 have two cross-sections closest to the impeller region, and there are four main vortices in the figure. The four vortices are centered symmetrically with respect to the position of the impeller, and with the increase of the number of revolutions, the fluid flow velocity increases, the turbulence intensifies, and the formation range and value of the vortex gradually decreases while the position of the vortex remains the same.

As shown in Fig. 3-8 and Fig. 3-9, the vortex range gradually decreases as the number of revolutions increases, but the vorticity value gradually increases in the cross-section away from the impeller. The farther away from the impeller cross-section, the more disordered the vortex becomes, and the range is unstable, and the direction of movement changes from transverse to longitudinal.

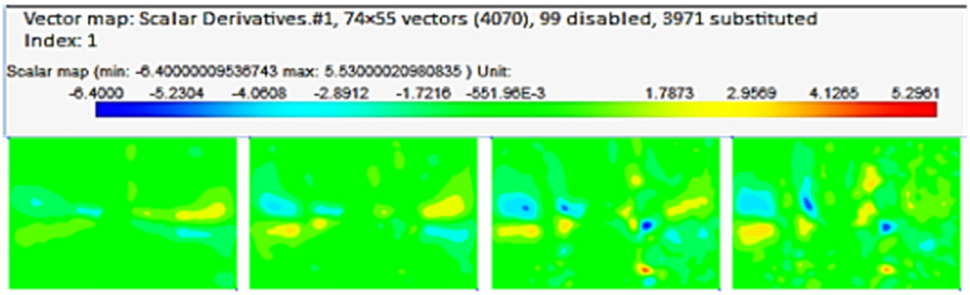

Figure 5. 0-0 Cross-section vorticity

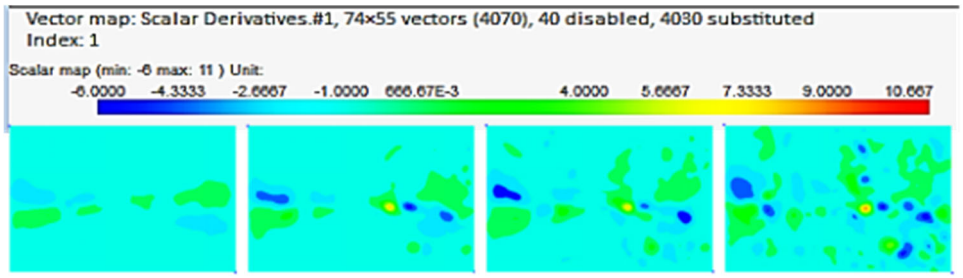

Figure 6. 20-20 Cross-section vorticity

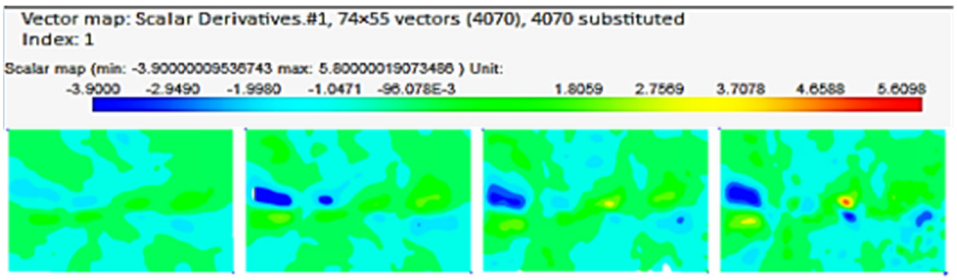

Figure 7. 40-40Cross-section vorticity

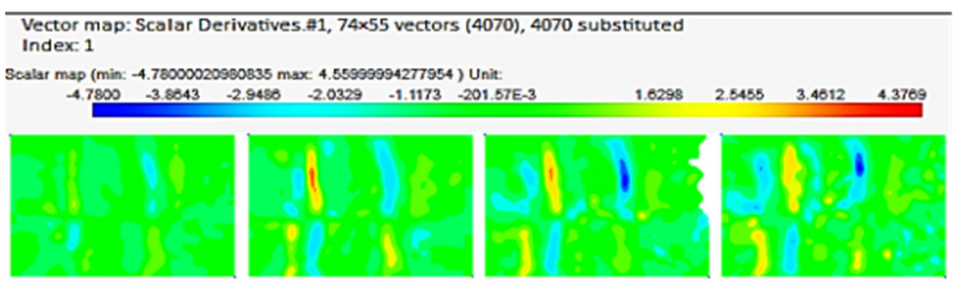

Figure 8. 60-60Cross-section vorticity

A histogram of the percentage of vorticity intensity in the 0-0 section is established, and it can be seen from Figure 3-10 that the vorticity value is symmetrical with respect to the vorticity intensity S=0.

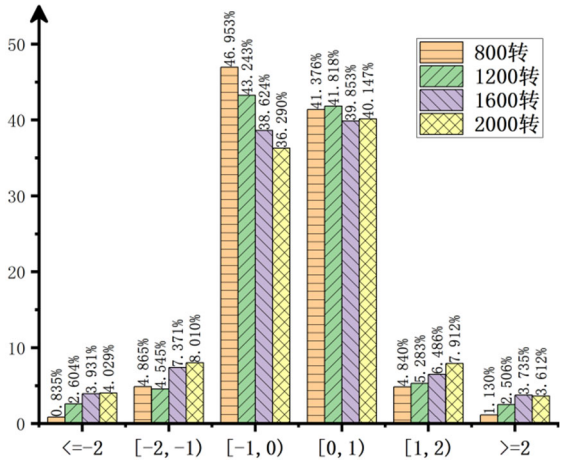

Figure 9. 0-0Percentage histogram of cross-section strength

The distribution curve was fitted to obtain the trend of "normal distribution curve", and the function was selected for curve fitting, and the function fitting formula is as follows:

$$y(x) = y_0 + \frac{2A}{\pi}\frac{w}{4(x-x_c)^2 + w^2} \tag{1}$$

The trend of the fitting curves is consistent with the experimental data, and they all show a "normal distribution", with a relative frequency fitting curve for the vorticity at 0-0 cross-section and rotational speed, as shown in Fig. 10.

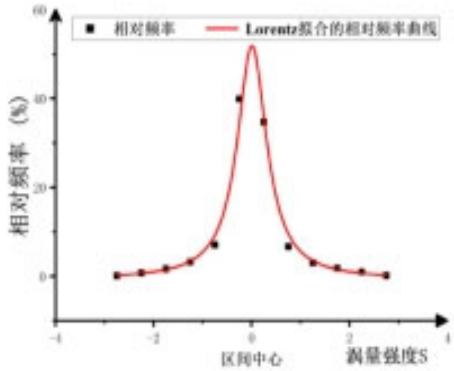

Figure 10. Lorentz curve

The data $y0$, x_c , w , A were analyzed and fitted, where the third-order polynomial was used for fitting and the formula was as follows:

$$y(x) = A + Bx + Cx^2 + Dx^3 \tag{2}$$

For linear fit, the formula is as follows:

$$y(x) = A + Bx \tag{3}$$

After the data fitting of the computer software, the $Lorentz$ parameters of the function are the functions about the variables, where is the rotational speed of the impeller, and the fitting function of each parameter in the 0-0 section is as follows:

$$y_{01} = -2.15802 + 0.00279x - 1.25*10^{-6}x^2 + 1.69*10^{-10}x^3 \tag{4}$$

$$x_{c1}(x) = -0.24335 + 6.57*10^{-4}x - 5.37*10^{-7}x^2 + 1.37*10^{-10}x^3 \tag{5}$$

$$w_1(x) = 0.46661 + 3.25*10^{-4}x \tag{6}$$

$$A_1(x) = 75.02732 - 0.03045x + 1.78*10^{-5}x^2 - 3.46*10^{-9}x^3 \tag{7}$$

Finally, the relationship between the vorticity in the 0-0 cross-section with respect to the speed of the impeller is obtained:

$$y(x) = -2.15802 + 0.00279x - 1.25*10^{-6}x^2 + 1.69*10^{-10}x^3 + \left[\frac{69.9404678 + 2.0341878*10^{-2}x - 3.187684*10^{-6}x^2 + 1.157*10^{-8}x^3 - 2.249*10^{-13}x^4}{\pi(0.45449377 + 1.94555x + 3.994744x^2 + 4.29316*10^{-4}x^3 - 1.09424*10^{-11}x^4 - 5.88552*10^{-17}x^5 + 7.5076*10^{-20}x^6)}\right]$$

3.2. The influence of rotational speed on the circulating flow rate of the flotation cell

In order to explore the circulating flow rate of the LZFD flotation cell, the data point analysis was carried out at the 0-0 section that is convenient for the measurement data, and the extracted data curve was analyzed in the Origin 2021 software to obtain the average curve, and the definite integral median value theorem was used.

The formula for the median value of the definite integral:

$$f(\xi) = \frac{1}{b-a}\int_a^b f(x)dx \tag{8}$$

In the experimentally extracted data, $\Delta = b - a = -116.7 - (-12.2) = -104.5mm$, The curves are integrated to obtain the area and average velocity.

Further fitting the obtained average velocity data with respect to the number of revolutions, the function adopts a second-order polynomial:

$$u(x) = A + Bx + Cx^2 \tag{9}$$

The fitting result of the fluid velocity function is:

$$u(x) = -0.04515 + 1.13*10^{-4}x - 3.60*10^{-8}x^2 \tag{10}$$

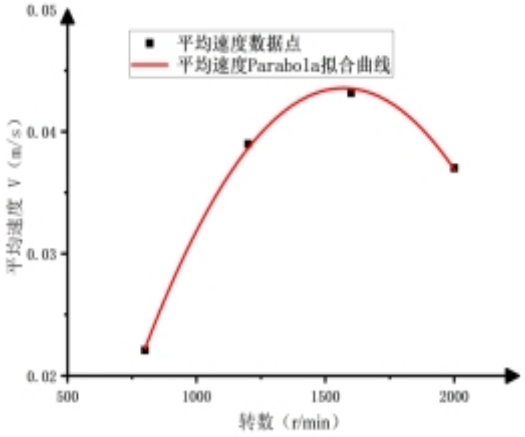

Figure 11. The average speed varies with the number of revolutions

Figure.11 shows the fitting curve. The volume flow function of the LZFD flotation cell with respect to the number of revolutions is obtained:

$$Vs(x) = u(x) * \pi Ra^2 * 3600 \tag{11}$$

Where Ra is the radius of the circulating flow region containing bubbles,Ra=116.7mm.

The measured nominal volume flow results are shown in Table 1.

Table 1. Date processing result

Rotate speed(r/min)	800	1200	1600	2000
Area($m^2 \cdot 10^{-2}$)	2.3094	4.07366	4.51102	3.86828
average velocity(m/s)	0.0221	0.03898	0.04317	0.03702
volume flow rate(m^3/h)	3.4039	6.0043	6.64894	5.70159

According to Eq. (10), the number of revolutions corresponding to the maximum value of the number of revolutions:

$$n = -\frac{b}{2a} = -\frac{1.13*10^4}{2*3.6} = 1569.44 r/\min \tag{12}$$

Put（$x = 1500 r/\min$）into（10）and（11）:

$u = 0.04335 m/s$

$Vs = 6.67703 m^3/h$

In this experiment, the theoretical optimal speed of the impeller of the LZFD flotation cell can be selected as 1500 r/min.

As shown in Table 1, the impeller speed has a maximum volume flow rate of $1600 r/\min$, which contributes to the efficiency of flotation of minerals. However, in the selection of flotation machine speed, it must also be considered that the greater the speed of the flotation engine impeller, the greater the resistance during its rotation, and under the condition of maintaining the maximum flow rate, it is necessary to choose a more economical engine output power, save more electrical energy, and reduce production costs. Therefore, it is possible to select a speed slightly lower than the maximum flow rate.

4. Conclusion

By studying the characteristics of the stirring flow field of the flotation cell, the following main conclusions are drawn:

(1) In the LZFD flotation machine, the vertical surface of the flow field can be divided into four areas from the bottom to the top according to the flow of the flow field. $H = 0 \sim 100mm$ is a mixed area of ore grains, and the fluid in this area is mainly horizontal; $H = 100 \sim 120mm$ is the mixing collision zone, which is close to the impeller mixing center area, where the ore particles and air bubbles collide violently; $H = 120 \sim 150mm$ is the bubble entry area, and the flow form of this area is dominated by the circulating flow of bubbles. $H = 200 \sim 240mm$ It is a foam stratosphere, and the flow velocity in this area is minimal.

(2) The flow field of the flotation cell can also divide the flow area into three zones from the periphery of the flow field to the center of the impeller agitation. The part close to the impeller is the collision area of upper and lower convection; Slightly away from the impeller area is a mixed area of circulating and rotary flow; The area away from the impeller exists in the form of a rotational flow and an upwelling flow.

(3) The calculation of the flow rate of the flotation cell and the fitting of the average speed of the impeller can theoretically select the optimal speed for the flotation machine and provide the best flow field for the flotation of the flotation machine is 1500 r/min.

Acknowledgment

Supported by The Innovation Fund of Postgraduate, Sichuan University of Science & Engineering. (Y2022050)

References

[1] Shen Zhengchang. The development history and development trend of flotation machine [J]. Non-ferrous metals (beneficiation), 2011 (S1):34-46.

[2] Sui Jiefei, He dongsheng, Li Zhili, et al. Application status and prospect of flotation machine[J/OL].Chemical Minerals & Processing, 2021.

[3] Wang Xiaoli, Wang Xiao, Liu Ze, et al. Optimized design of XFD single-tank flotation cell for laboratory use[J].Resources, Environment and Engineering, 2020, 34(S1): 129-131.

[4] Kong Weibo. Application and development of PIV technology [J]. Shandong Chemical, 2019 (6): 115-115+119.

[5] Li Hongfei,Song Wenwu. Application of PIV technology in flow testing and research [J]. Journal of Xihua University: Natural Science Edition, 2009, 28(5): 27-31.

[6] Gong Zhijun, Wu Wenfei, Zhao Zengwu, et al. PIV technology was used to study the flow characteristics in the stirring tank [J]. Journal of Baotou Iron and Steel Institute, 2005, 24(2):133-136.

[7] Liu Bing, Cui Lishui, Li Xiaoting, et al. Analysis of influencing factors of measurement accuracy of particle image velocimetry [J]. Journal of Metrology,2021,42(3):346-351.

[8] Li Nan, Xie Gang, Shi Zhe,et al. Analysis of flow field characteristics of XFD flotation machine based on laser PIV technology [J]. Optoelectronics and lasers, 2015, 26(03): 586-591.

[9] DruaultP, GuibertP, AlizonF. Useofproperorthogonal cecompositionfortime interpolationfrom PIV data[J] ExperimentsinFluids, 2005, 39(6): 1009—1023.